

Morphotectonic Analysis between Crete and Kasos

D. Lampridou¹, P. Nomikou¹, M. Alexandri, D. Papanikolaou¹, C. Hübscher²,
Th. Ioannou¹, P. Sorotou¹ and L. Ragia³

¹*Department of Geology and Geoenvironment, National and Kapodistrian University of Athens,
Panepistimioupoli Zografou, 15784 Athens, Greece*

²*Institute of Geophysics, Center for Earth System Research and Sustainability, University of 11 Hamburg,
Bundesstraße. 55, D-20146 Hamburg, Germany*

³*Natural Hazards, Tsunami and Coastal Engineering Laboratory, Technical University of Crete, Chania, Greece*

Keywords: Swath Bathymetry, Crete and Kasos, Morphotectonic Analysis.

Abstract: The morphotectonic structure of the offshore area lying between Crete and Kasos is studied on the basis of new detailed bathymetric data. The resulting bathymetric map is presented. Qualitative analysis of morphological slope values, as well as the analysis of the watershed at the eastern part of Crete, confirms that the current seabed topographic relief reflects intense tectonic activity. The high morphological slope values indicate well-defined morphotectonic features, which mainly trend SW-NE and, secondarily, SSW-NNE. The main large-scale tectonic structures trend SW-NE correspond to the marginal faults that bound the Crete-Kasos basin. The overall basin geometry is an elongated rectangular which is divided into seven sub-basins, and the deepest one (2800m) is located at the eastern part of the area. Moreover, the complex regime of the seafloor includes submarine canyons, landslides and a well-defined slump with vertical displacement more than 400m.

1 INTRODUCTION

The importance for improving our understanding of geohazards is evident from global events. Globally, disasters affected 150 million people and inflicted an estimated damage of US\$ 100-150 billion over a few years as documented by various reports (<http://www.unisdr.org>).

Kvalstad (2007) defined geohazard in the offshore domain, as “local and/or regional site and soil conditions having a potential of developing into failure events causing loss of life or damage to health, environment or field installations”. Examples of such hazards include earthquakes and submarine landslides, iceberg scouring of the seabed, and gas migration that can lead to locally overpressurized sediments and potential terrain instability and/or blowouts (Fig.1). Secondary effects such as tsunamis (either triggered by earthquakes or landslides) also need to be considered, as both their genesis and propagation are strongly controlled by seafloor morphology (Chiocci et al., 2011). Hence, there is an urgent need to determine better the development of geohazards and inherent risks, and an adequate response to them. This need is also accentuated by

the increased vulnerability of coastal areas to earthquakes because of rapid growth of urban centres.

Tsunamis are a low frequency natural hazard with potentially catastrophic consequences. The knowledge of their recurrence is of critical importance for the development of models and scenarios adapted to local and regional conditions, thus giving support to the design of warning systems and mitigation measures.

The Hellenic subduction zone (HSZ) has historically generated among the most devastating earthquakes, and by far the most damaging tsunamis in the entire Mediterranean region. Historic earthquakes along the HSZ, particularly along the Crete segment, attest to some degree of coupling on the plate interface (Shaw et al., 2008; Guidoboni and Comastri, 1997; England et al., 2015).

To properly assess and describe hazards complexity and manageability it is required an understanding of the broader geologic, sedimentary and tectonic variability. Therefore, multi-disciplinary surveys aimed at detecting and mapping geohazards, are being conducted.

The advent of multibeam sonar (MBS) technology has allowed imaging of the seafloor with unparalleled resolution, spatial coverage and

precision and today offer the most cost effective way to explore the ocean floor (Hughes et al. 1996, Chiocci et al. 2011).

High resolution swath data obtained during oceanographic cruise in the framework of FP7 “ASTARTE: Assessment, Strategy and Risk Reduction for Tsunamis in Europe-ASTARTE” project in the South Aegean Sea. The aim of this paper has been the fault recognition by applying morphostructural analysis, which was based on the quantitative interpretation of the seafloor topography, the slope distribution and the drainage pattern development in the offshore area lying between Crete and Kasos.

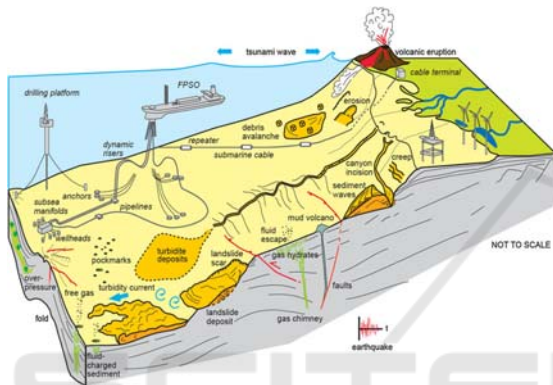


Figure 1: Cartoon summarizing the seafloor features linked to potentially hazardous geological processes (Chiocci et al., 2011).

2 REGIONAL SETTING

The Hellenic subduction zone is the largest, fastest and most seismically active subduction zone in the Mediterranean, where the African slab subducts beneath Crete at a rate of $\sim 36 \text{ mm yr}^{-1}$ (McClusky et al., 2000; Reilinger et al., 2006). The subduction rate greatly exceeds the convergence between Africa (Nubia) and Eurasia ($5\text{-}10 \text{ mm yr}^{-1}$) because of the rapid SW motion of the southern Aegean itself, relative to Eurasia (McKenzie 1972; Reilinger et al., 2006). The surface morphology of the subduction system is obscured beneath a sedimentary section up to 10 km thick overlying the ocean crust, which is deformed in a broad accretionary prism south of Crete, known as the Mediterranean Ridge accretionary complex $\sim 150 \text{ km}$ south of Crete (Le Pichon et al. 1979, Kastens, 1991, Chamot-Rooke et al., 2004). A dramatic 2-3 km high, south-facing bathymetric scarp extends in an arc between the Peloponnese and Crete, splitting into three branches

south of Crete, and continuing east up to Rhodes constituting Ptolemy, Pliny and Strabo trenches (McKenzie 1978; Le Pichon et al. 1979). Although this scarp is referred as the Hellenic Trench, the southern margin of the continental Aegean lithosphere is located about 100 km south of the Cretan coast (Bohnhoff et al., 2001) and it is possible to follow the subduction zone through a well-defined Benioff zone to a depth of 150-180 km below the central Aegean Sea (Papazachos et al., 2000). The Ptolemy, Strabo and Pliny Trenches, despite their names, are not trenches in the plate-tectonic sense but probably represent the outcrop of major faults within the deforming sedimentary wedge on top of the Nubian plate (Shaw et al., 2008; Shaw, B., Jackson, J., 2010, Huguen et al., 2001; Le Pichon X, Angelier J. 1979; Kreemer C, Chamot-Rooke N. 2004; Mascle et al., 1986; McKenzie 1978; Gallen et al., 2104). While the Hellenic Trench is generally considered to represent the outcrop of a reverse fault, the Pliny and Strabo Trenches have been interpreted as the expressions of normal faulting ([Gallen et al., 2014), strike-slip faulting (Mascle et al., 1982; Ozbakir et al., 2013), reverse faulting (Shaw and Jackson, 2010; Jongsma 1977) and various combinations of these (e.g. Huguen et al., 2001; Mascle et al 1986, Peters and Huson 1985; tenVenn et al., 2009).

Nowadays, the Hellenic arc is associated with moderate arc-parallel extension and strong compression perpendicular to it (Kahle et al., 1998). The geometry of tectonic troughs offshore Crete reflects a two-tier deformation mechanism at depth, in which oblique extension predominates in the upper 10-15 km of the crust and oblique compression predominates underneath this limit (Kokkinou et al. 2012). This obliquity has been associated with rapid exhumation of basement units and intense uplift of the forearc region where Crete, Gavdos, Kasos and Karpathos islands are located (Le Pichon et al., 2002). The Hellenic Subduction Zone (HSZ) produced two $M \sim 8$ earthquakes, both near Crete, during the > 2000 year historic record, AD 365 and AD 1303 (Shaw et al., 2008; Guidoboni and Comastri, 1997; England et al., 2015). Both caused severe damage from shaking and the resulting tsunamis caused major damage around the Eastern Mediterranean. The precise locations and mechanisms of these ancient events are not well known. The AD 365 event is thought to have occurred on a splay fault extending from the plate interface towards the surface below southwestern Crete (Shaw et al., 2008). Large uplift recorded by shorelines in western Crete has been interpreted as due to coseismic slip on the splay fault. The location

of the AD 1303 event is constrained only from damage reports and is believed to be located near southeast Crete (Guidoboni and Comastri, 1997). Significantly, the AD 1303 event caused no observable shoreline uplift, although a substantial tsunami was well recorded (England et al., 2015). Noteworthy are the catastrophic events in AD 365 and AD 1303, during which Alexandria and the rest of the Nile Delta were flooded extensively by the tsunamis triggered by these events (Ambraseys 2009).

The offshore area between Crete and Kasos is characterised by the large number of poorly characterized bathymetric scarps that cross the region. Each of these is potentially associated with a fault capable of generating a rare, high-magnitude, earthquake. Unlike the other parts of the Hellenic plate boundary, however, there is no possibility of detecting past earthquakes from on-shore geological evidence. The principal faults lie far enough from the shore that no detectable uplift of shorelines would be expected (Howell et al. 2015), making a detailed marine survey essential.

According to England et al., 2015, the Pliny Trench is the most probable source of a tsunamigenic earthquake in HSZ. Nevertheless, large earthquakes occurring along Strabo and Ptolemy Trenches, can trigger tsunamis.

Although the Hellenic system represents the most significant seismic and tsunami hazard in the Mediterranean region, its kinematics and associated hazards remain uncertain because available GPS data are not sufficiently precise and spatially distributed to determine the distribution of strain accumulation on the plate boundary faults (England et al., 2015). Many important details of the kinematics-dynamics of the Hellenic subduction zone remain poorly understood and under debate.

3 METHODOLOGY

3.1 Data Acquisition

Data used in this paper have been obtained onboard R/V Med Surveyor in the framework of the research program “ASTARTE: Assessment, Strategy and Risk Reduction for Tsunamis in Europe-ASTARTE”. Swath bathymetry data were acquired using multibeam echosounder Elac’s SeaBeam 3030, which operates in the 30 kHz band and incorporates a multi-ping capability (two swaths per ping). Data were logged with HYPACK. The collected multibeam data have been extensively processed by means of data

editing, cleaning of erroneous beams, filtering of noise, processing of navigation data and interpolation of missing beams, using the open-source software MB-SYSTEM, and then gridded with grid spacing of 50m. Analyses and representation of bathymetric data were performed with ArcGIS 10.1 software and Global Mapper v.16.

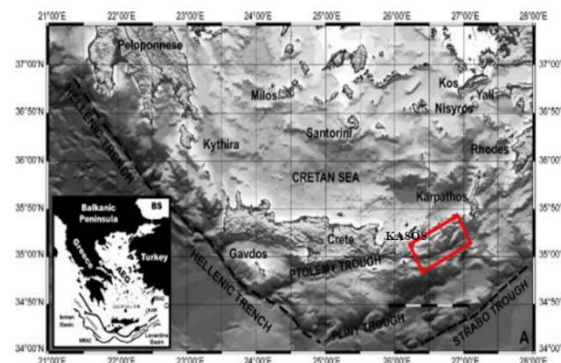


Figure 2: General map of the area (Kokinou et al., 2012), the red box corresponds to the study area.

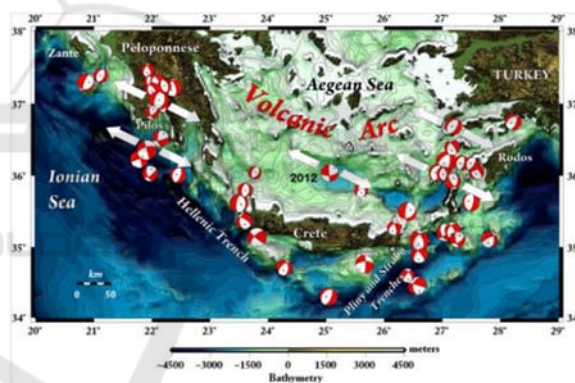


Figure 3: All earthquake focal mechanisms, with $M_w > 4.0$ and focal depths less than 25 km, are plotted which reflect the accommodation of extension within the material of the overriding southern Aegean Sea, above the subduction interface (Kiratzi, 2013).

3.2 Bathymetry Map

The resulting slope-shaded bathymetric map was compiled at 1:300,000 scale. This map permits a first description of the overall topography of the seafloor as well as the mapping of the major morphotectonic structures (Fig.4a).

3.3 Slope Map

The bathymetric map of the area was analysed as far as the slope distribution is concerned. The slope distribution map shows the distribution of slope

values within the study area distinguished in four categories a) areas of mean morphological slope 0° - 5° , b) areas of 5° - 20° , c) areas of 20° - 40° d) and areas of $>40^{\circ}$. This classification of the slope magnitude will illustrate the zones where there is an abrupt change of slope, reflecting possible positions of active tectonic zones in contrast with zones with negligible change of slope, which reflect flat-lying areas such as submarine terraces or basinal areas (Fig.4b).

3.4 Slope-aspect Map

The combined slope-aspect map captures both the direction of the slopes and their steepness, illustrating the overall geometry of the area and changes in the relief orientation which may be attributed to active tectonic structures. The direction of the slope (degrees) is expressed in hue and the steepness of the slope (degrees) is expressed by its saturation (Fig.4c).

3.5 Watershed

Submarine canyons, small gullies and stream network were extracted for the entire area employing the in-built hydrology tools. When extracting the drainage pattern the following points have to be taken into account : a) the flow accumulation output grid was produced by applying a threshold upstream cell number of 200, b) multibeam artefacts can result in the interruption of streams or the generation of spurious ones.

4 RESULTS

Synthetic Morphotectonic Map of the under study area was carried out by means of the combined use of: (a) Seabed Digital Elevation Model (SDEM), (b) Slope Distribution Map, (c) Slope-aspect Map and (d) Drainage Pattern Map. The composition of the digital modelling in conjunction with the regional geodynamic setting, allows the identification of the main morphological discontinuities and lineaments that result from morphotectonic.

The bathymetric map reveals a rather rough seafloor topography where flat-lying areas alternate with rough morphology. Two prominent fault zones form the general structure of the area. The first fault zone strikes SW-NE comprising the marginal faults that delineate the central subsided area. The second fault zone, strikes SSW-NNE and crosscuts the first one. The topographic difference along the marginal

faults, which apparently correlates with the fault throw, ranges between 1200m up to 1500m. The northern marginal fault presents its greater topographic difference at the western and far eastern part, while the southern marginal fault at its eastern part. This is possibly linked to the different structural deformation of the area. The basinal area that is bounded by the previous SW-NE identified fault zone, is divided into seven elongated sub-basins, parallel to the alignment of the marginal faults. The sub-basins are lying at 2200m, 2500m, 2600m and 2800 water depths respectively. The eastern basin is a simple geometric basin with a flat-lying sea bottom (2800m) at the junction of the two major marginal fault zones, and its maximum subsidence is accommodated by the southern marginal fault. The western part of the basin has a very complex topographic regime carved by several sub-basins developed with different geometric shapes at different water depths and separated by distinct intermediate submarine ridge with topographic differences ranging from 150m of meters.

Numerous gullies that dissect the slopes, trending almost NW-SE, coalesce at several depths ending up at the seven sub-basins. The most prominent submarine canyon is the one bounded by the secondary fault zone that strikes SSW-NNE. Its a U-shaped rather linear feature and its thalweg depth ranges between 1300m and 2800m water depth. The channel walls are asymmetrical and the axis profile displays a linear morphology (Fig.5).

Submarine landslides were also identified in the study area by the typical crescent-shape scar. The most interesting is the one comprising the NW flank of the linear channel. It is a typical slump with four distinguishable «steps» at 1500m, 1600m, 1700m 1800m, meaning that the vertical displacement is approximately 100m. Noteworthy is that this kind of landslides can trigger tsunamis.

5 CONCLUSIONS

The morphotectonic interpretation, accomplished by the compilation of the previously presented maps in combination with the multichannel seismic profiles acquired during the project, has led to the construction of the Morphotectonic map (Fig.6).

The Crete – Kasos studied area comprises a more than 50km long basin in the ENE-WSW direction with an average width of 10km. This basin forms a tectonic graben bounded by two sub-parallel marginal fault zones, which have produced a relative subsidence of more than 1200m of the basinal area.

The sea bottom of the basin is complicated with seven sub-basins elongated in the ENE-WSW direction separated by intermediate ridges not surpassing 150m of relative relief. The sea bottom at the eastern larger basin occurs at a depth of 2800m. Along the shallow slopes of the two marginal fault zones outside the basin a large number of submarine canyons and landslides occur as well as a slumped area of 20X30km at the northern margin, whose overall vertical displacement seems to exceed 400m. The two ENE-WSW marginal faults form two broad zones of a few km width along their dip towards the subsided zone with topographic differences ranging between 1300 and 1500m. Several sub-parallel faults are observed within the basin, which form an intermediate ridge/horst along the axis of the tectonic graben. These faults might represent antithetic faults to the major marginal faults of the graben. Outside the basin/graben the observed faults show a NE-SW orientation with a prominent elongated tectonic valley/graben at the eastern part, which seems to affect also the continuity of the northern marginal fault towards the ENE. The topographic effect of the two marginal faults is different along their strike with maximum cliff observed at the western part of the northern fault whereas the maximum cliff of the southern fault is observed at the eastern part. The above narrow tectonic zone/graben of the studied area between Crete and Kasos corresponds to the eastern prolongation of the Ptolemy trench, which is observed from the southern slopes of Gavdos to those of eastern Crete. The overall tectonic structure resembles a transtensive regime with oblique normal faulting combining an opening in the NW-SE direction together with a left-lateral strike slip motion, which is supported also by earthquake mechanisms.

ACKNOWLEDGEMENTS

This work was supported and funded by the FP7 "ASTARTE: Assessment, Strategy and Risk Reduction for Tsunamis in Europe-ASTARTE".

We are grateful to Costas Synolakis and Philip England for their beneficial contribution and comments.

REFERENCES

- Ambraseys, N.N. (2009) Earthquakes in the Mediterranean and middle east: *A Multidisciplinary study of Seismicity up to 1900*. Nicholas Ambraseys. Cambridge, UK: Cambridge University Press.
- Bohnhoff, M., Makris, J., Papanikolaou, D. and Stavrakakis, G. (2001) 'Crustal investigation of the Hellenic subduction zone using wide aperture seismic data', *Tectonophysics*, 343(3-4), pp. 239–262. doi: 10.1016/s0040-1951(01)00264-5.
- Chiocci, F.L., Cattaneo, A. and Urgeles, R. (2011) 'Seafloor mapping for geohazard assessment: State of the art', *Marine Geophysical Research*, 32(1-2), pp. 1–11. doi: 10.1007/s11001-011-9139-8.
- England, P., Howell, A., Jackson, J., Synolakis, C., 2015. Palaeotsunamis and tsunami hazards in the *Eastern Mediterranean*. *Philosophical Transactions of the Royal Society A: Mathematical, Physical and Engineering Sciences* 373, 20140374. doi:10.1098/rsta.2014.037.
- Gallen, S., Wegmann, K., Bohnenstiehl, D., Pazzaglia, F., Brandon, M., Fassoulas, C., 2014. Active simultaneous uplift and margin-normal extension in a forearc high, Crete, Greece. *Earth and Planetary Science Letters* 398, 11–24. doi:10.1016/j.epsl.2014.04.038.
- Guidoboni, E., Comastri, A., 1997. *Journal of Seismology*. *Journal of Seismology* 1, pp. 55–72. doi:10.1023/a:1009737632542.
- Howell, A., Jackson, J., England, P., Higham, T., Synolakis, C., 2015. Late Holocene uplift of Rhodes, Greece: evidence for a large tsunamigenic earthquake and the implications for the tectonics of the eastern Hellenic Trench System. *Geophysical Journal International* 203, pp.459–474. doi:10.1093/gji/ggv307.
- Huguen, C., Mascle, J., Chaumillon, E., Kopf, A., Woodside, J., Zitter, T., 2004. Structural setting and tectonic control of mud volcanoes from the Central Mediterranean Ridge (Eastern Mediterranean). *Marine Geology* 209, pp. 245–263. doi:10.1016/j.margeo.2004.05.002.
- Hughes Clarke, J.E., Mayer, L.A. and Wells, D.E. (1996) 'Shallow-water imaging multibeam sonars: A new tool for investigating seafloor processes in the coastal zone and on the continental shelf', *Marine Geophysical Researches*, 18(6), pp. 607–629. doi: 10.1007/bf00313877.
- Jongsma, D. (1977) 'Bathymetry and shallow structure of the Pliny and Strabo "trenches", south of the Hellenic Arc'. *Geol.Soc.Am.Bull.*88, pp. 797–805. doi:10.1130/00167606(1977)88<797:-BASSOT>2.0.CO;2.
- Kahle, H.-G., Straub, C., Reilinger, R., McClusky, S., King, R., Hurst, K., Veis, G., Kastens, K. and Cross, P. (1998) 'The strain rate field in the eastern Mediterranean region, estimated by repeated GPS measurements', *Tectonophysics*, 294(3-4), pp. 237–252. doi: 10.1016/s0040-1951(98)00102-4.
- Kastens, K.A. (1991) 'Rate of outward growth of the Mediterranean ridge accretionary complex' *Tectonophysics* 199, pp 25-50. doi: 10.1016/0040-1951(91)90117-B.

- Kiratzi, A., 2013. The January 2012 earthquake sequence in the Cretan Basin, south of the Hellenic Volcanic Arc: Focal mechanisms, rupture directivity and slip models. *Tectonophysics* 586, pp.160–172. doi:10.1016/j.tecto.2012.11.019.
- Kokinou, E., Tiago, A., Evangelos, K. and ekokinou (2012) 'Structural decoupling in a convergent forearc setting (southern Crete, eastern Mediterranean)', *Geological Society of America Bulletin*, 124(7-8), pp. 1352–1364. doi: 10.1130/B30492.1.
- Kreemer, C., de Géologie, L., supérieure, E. normale, Paris, Chamot-Rooke, N. and 8538, C.U. (2004) 'Contemporary kinematics of the southern Aegean and the Mediterranean ridge', *Geophysical Journal International*, 157(3), pp. 1377–1392. doi: 10.1111/j.1365-246X.2004.02270.x.
- Kvalstad, T.J. (2007) 'What is the current "best practice" in offshore Geohazard investigations? A state-of-the-art review'. doi: 10.4043/18545-MS.
- Le Pichon, X., Angelier, J., Aubouin, J., Lyberis, N., Monti, S., Renard, V., Got, H., Hsu", K., Mart, Y., Mascle, J., Matthews, D., Mitropoulos, D., Tsoflias, P. and Chronis, G. (1979) 'From subduction to transform motion: A seabeam survey of the Hellenic trench system', *Earth and Planetary Science Letters*, 44(3), pp. 441–450. doi: 10.1016/0012-821x(79)90082-7.
- Le Pichon, X., Lallemand, S.J., Chamot-Rooke, N., Lemeur, D. and Pascal, G. (2002) 'The Mediterranean ridge backstop and the Hellenic nappes', *Marine Geology*, 186(1-2), pp. 111–125. doi: 10.1016/s0025-3227(02)00175-5.
- Mascle, J., Jongsma, D., Campredon, R., Dercourt, J., Glaçon, G., Leclach, A., Lybéris, N., Malod, J., Mitropoulos, D., 1982. The Hellenic margin from eastern Crete to Rhodes: Preliminary results. *Tectonophysics* 86, pp.133–147. doi:10.1016/0040-1951(82)90064-6.
- Mascle, J., Cleac'h, A., Jongsma, D., 1986. The eastern Hellenic margin from Crete to Rhodes: Example of progressive collision. *Marine Geology* 73, pp.145–168. doi:10.1016/0025-3227(86)90116-7.
- McClusky, S., Balassanian, S., Barka, A., Demir, C., Ergintav, S., Georgiev, I., Gurkan, O., Hamburger, M., Hurst, K., Kahle, H., Kastens, K., Kekelidze, G., King, R., Kotzev, V., Lenk, O., Mahmoud, S., Mishin, A., Nadariya, M., Ouzounis, A., Paradissis, D., Peter, Y., Prilepin, M., Reilinger, R., Sanli, I., Seeger, H., Tealeb, A., Toksöz, M.N. and Veis, G. (2000) 'Global positioning system constraints on plate kinematics and dynamics in the eastern Mediterranean and Caucasus', *Journal of Geophysical Research: Solid Earth*, 105(B3), pp. 5695–5719. doi: 10.1029/1999jb900351.
- McKenzie, D. (1972) 'Active Tectonics of the Mediterranean region', *Geophysical Journal International*, 30(2), pp. 109–185. doi: 10.1111/j.1365-246x.1972.tb02351.x.
- McKenzie, D. (1978) 'Active tectonics of the Alpine-Himalayan belt: The Aegean sea and surrounding regions', *Geophysical Journal International*, 55(1), pp. 217–254. doi: 10.1111/j.1365-246x.1978.tb04759.x.
- Özbakır, A.D., Şengör, A., Wortel, M., Govers, R., 2013. The Pliny–Strabo trench region: A large shear zone resulting from slab tearing. *Earth and Planetary Science Letters* 375, pp.188–195. doi:10.1016/j.epsl.2013.05.025.
- Papazachos, B.C., Karakostas, V.G., Papazachos, C.B. and Scordilis, E.M. (2000) 'The geometry of the Wadati–Benioff zone and lithospheric kinematics in the Hellenic arc', *Tectonophysics*, 319(4), pp. 275–300. doi: 10.1016/s0040-1951(99)00299-1.
- Peters, J., Huson, W., 1985. The Pliny and Strabo trenches (eastern Mediterranean): Integration of seismic reflection data and SeaBeam bathymetric maps. *Marine Geology* 64, pp.1–17. doi:10.1016/0025-3227(85)90157-4.
- Reilinger, R., McClusky, S., Vernant, P., Lawrence, S., Ergintav, S., Cakmak, R., Ozener, H., Kadirov, F., Guliev, I., Stepanyan, R., Nadariya, M., Hahubia, G., Mahmoud, S., Sakr, K., ArRajehi, A., Paradissis, D., Al-Aydrus, A., Prilepin, M., Guseva, T., Evren, E., Dmitrotsa, A., Filikov, S.V., Gomez, F., Al-Ghazzi, R. and Karam, G. (2006) 'GPS constraints on continental deformation in the Africa-Arabia-Eurasia continental collision zone and implications for the dynamics of plate interactions', *Journal of Geophysical Research: Solid Earth*, 111(B5), doi: 10.1029/2005jb004051.
- Shaw, B., Ambraseys, N.N., England, P.C., Floyd, M.A., Gorman, G.J., Higham, T.F.G., Jackson, J.A., Nocquet, J.-M., Pain, C.C., Piggott, M.D., (2008). Eastern Mediterranean tectonics and tsunami hazard inferred from the AD 365 earthquake. *Nature Geoscience* 1, pp. 268–276. doi:10.1038/ngeo151.
- Shaw, B., Jackson, J., 2010. Earthquake mechanisms and active tectonics of the Hellenic subduction zone. *Geophysical Journal International*. doi:10.1111/j.1365-246x.2010.04551.x.
- Veen, J.T., Boulton, S., Alçiçek, M., 2009. From palaeotectonics to neotectonics in the Neotethys realm: The importance of kinematic decoupling and inherited structural grain in SW Anatolia (Turkey). *Tectonophysics* 473, pp.261–281. doi:10.1016/j.tecto.2008.09.030.

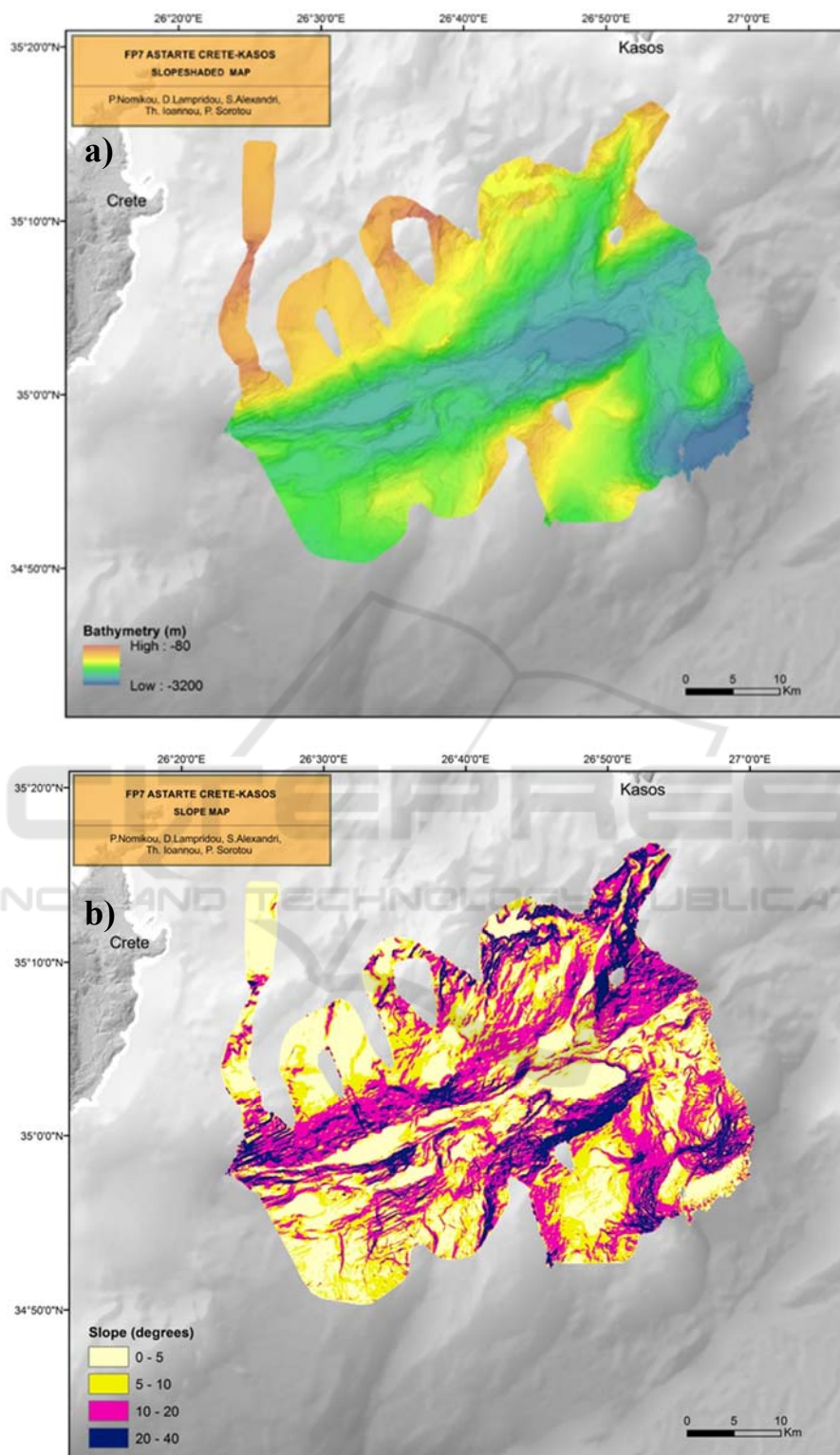


Figure 4: a) Bathymetry map, b) Slope map, c) Slope-Aspect map.

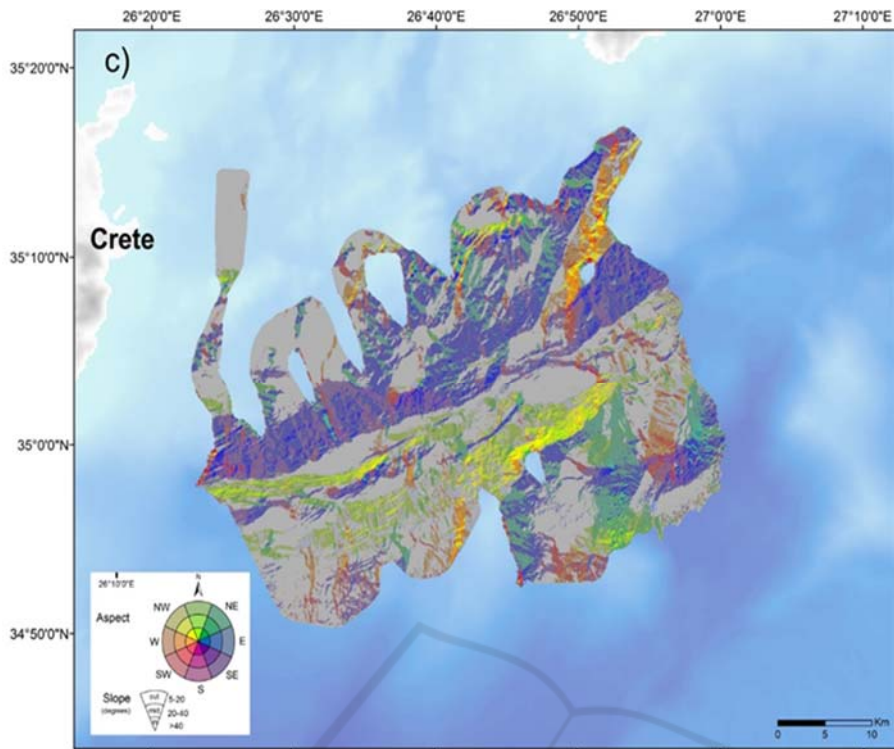


Figure 4: a) Bathymetry map, b) Slope map, c) Slope-Aspect map (cont.).

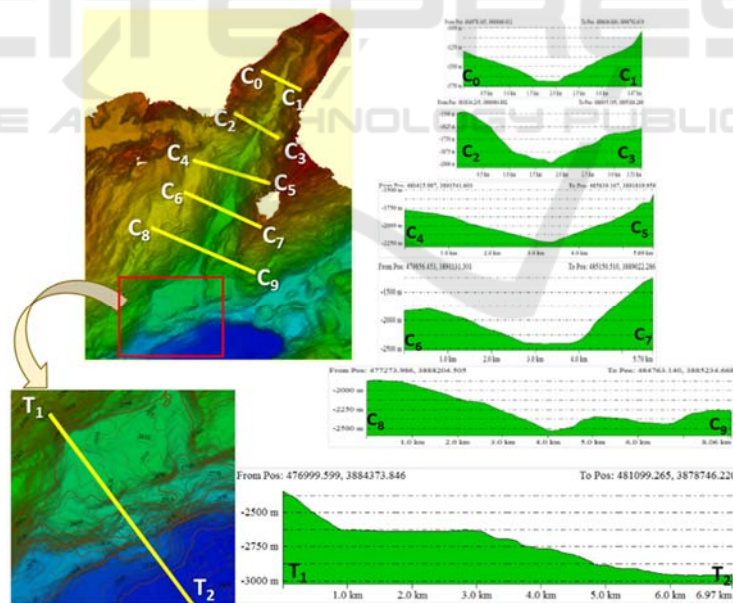


Figure 5: Detailed view of the Kasos canyon with the location of the cross sections. a. C0-C9 vertical topographic sections perpendicular to canyon axis, b. Detailed view and topographic section (T1-T2) at the end of canyon.

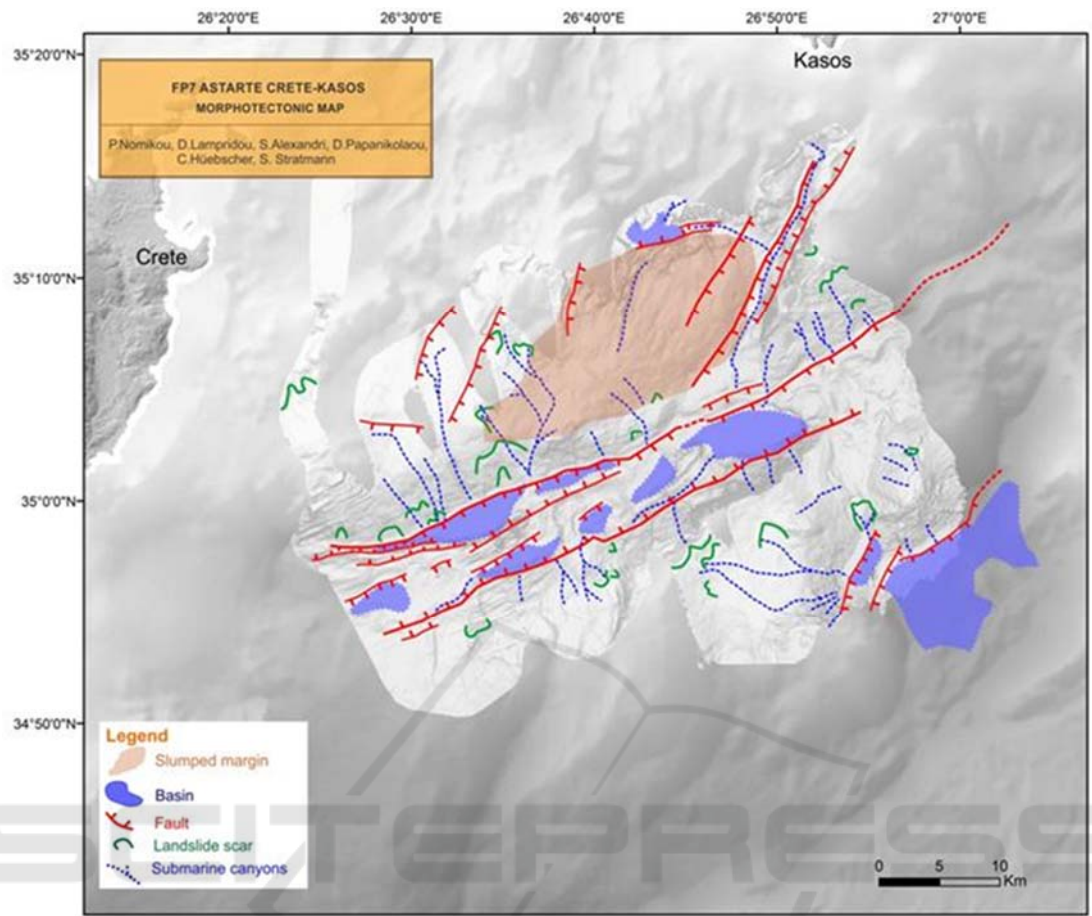


Figure 6: Morphotectonic map.